This is the accepted manuscript made available via CHORUS. The article has been published as:

# Imaging of magnetoplasmons excited in a two-dimensional electron gas

I. Baskin, B. M. Ashkinadze, E. Cohen, and L. N. Pfeiffer

Phys. Rev. B **84**, 041305 — Published 20 July 2011

DOI: 10.1103/PhysRevB.84.041305

# Imaging of magnetoplasmons excited in a two-dimensional electron gas

I. Baskin, B. M. Ashkinadze, E. Cohen
*Solid State Institute, Technion-Israel Institute of Technology, Haifa 32000, Israel*

L. N. Pfeiffer
*Department of Electrical Engineering, Princeton University, Princeton, NJ 08544, USA*

We report on the direct observation of magnetoplasmon modes that are excited in a laterally-confined two dimensional electron gas (2DEG) by microwave radiation. The magnetoplasmon-polaritons were imaged using spatially resolved photoluminescence (PL) spectroscopy of GaAs heterostructures, and their dependence on an external magnetic field and 2DEG density were studied. The PL pattern formation originates in the PL spectrum modulation by electrons that are heated by the local electric field of the magnetoplasmons. We revealed remarkable spatial oscillations of the microwave electric field in the samples containing a high mobility 2DEG.

PACS numbers: 73.50.Mx;78.70.Gq;73.20.Mf
Keywords: two dimensional electron gas, Magnetoplasmons, microwaves, photoluminescence, hot electrons

The plasma oscillations in a two-dimensional electron gas (2DEG) are discribed by the dispersion relation:[1]

$$\omega_p^2 = 2\pi n_{2d} e^2 q/\varepsilon m^* \tag{1}$$

Here, $\omega_p$ is the plasmon frequency, $n_{2d}$ and $m^*$ are the density and effective mass of the 2D-electrons, $\varepsilon \simeq (1+\varepsilon_{GaAs})/2$ is the effective dielectric constant and $q$ is the 2D-plasmon wave-vector. Under an external magnetic field $B$, applied perpendicularly to the 2DEG layer, the plasmons are transformed into the magnetoplasmons whose dispersion is:

$$\omega_{mp}^2 = \omega_p^2 + \omega_c^2 \tag{2}$$

where $\omega_c = eB/cm^*$ is the cyclotron frequency.

In finite-sized 2DEG systems (e.g. a strip of width $W$), an external electromagnetic radiation of frequency $\omega = \omega_{mp}$ excites confined plasmon/magnetoplasmon (MP) modes (standing wave oscillations)[2] with quantized values of $q \simeq N\pi/W$, where $N = 1, 2, \ldots$ . MP resonances of a 2DEG have been studied by far-infrared and microwave (mw) transmission spectroscopy of small mesa arrays,[3] Hall bars and quantum dots,[4,5] as well as of a single 2DEG disk.[6] MP's were also studied by optically detected resonance utilizing the heating of 2D-electrons by mw radiation in order to modulate the photoluminescence (PL) spectrum. The PL modulation is resonantly enhanced at the magnetoplasmon resonances, thus providing a sensitive detection of confined 2DEG-magnetoplasmons that are excited in 2D-disks, rings and stripes of various sizes.[9]

Interest in the physics of the 2DEG MP's has increased with the observation of mw induced resistance oscillations (MIRO), see references in[10]. In spite of extensive experimental and theoretical studies, the MIRO mechanism and the origin of zero-resistance states that emerge at high mw radiation power, remain unclear (see [10,11] and Refs. there). Recently, it has been suggested that MP's play a significant role in the MIRO mechanism.[11,12] Indeed, the MP modes excited in a laterally confined 2DEG, give rise to a spatially-nonuniform electric field $\varepsilon_{mp}$ that may affect the $B$-dependence of mw-induced resistance of the sample.[13]

Imaging of the $\varepsilon_{mp}$-distribution produced by the MP modes is a challenging task. To the best of our knowledge imaging the 2DEG plasmon electric field has not been accomplished yet. In modern plasmonics, plasmon mode imaging was performed using sophisticated subwavelength resolution techniques[14] such as, for example, single molecule fluorescence induced by plasmons.[15]

In this report we present the first observation of the spatial $\varepsilon_{mp}$-distribution in standing MP-polaritons modes (coupled mw and plasmon electric field oscillations). These modes are excited by microwaves in a laterally-confined high-mobility 2DEG in GaAs/AlGaAs heterostructures and are imaged by spatially-resolved PL spectroscopy. Optical imaging of MP modes originates in the local PL spectrum modulation by electrons heated in $\varepsilon_{mp}$. The MP pattern evolution with varying $n_{2d}$, $B$ and $\omega$ is studied.

The samples were prepared from various GaAs/AlGaAs wafers having heterostructures that contain a high-mobility 2DEG. Modulation doped quantum wells (MDQW) of various widths (20-70 nm-wide) and single heterojunctions (SHJ) were grown by molecular beam epitaxy on (001)-GaAs wafers. The measured 2DEG density and mobility were in the range of $n_{2d}$ = (0.2-2.0)$\cdot 10^{11}$ cm$^{-2}$ and $\mu_e$ = (2-15)$\cdot 10^6$ cm$^2$/V$\cdot$s, respectively. The sample bar (size of $\sim$ 1x4 mm$^2$) was placed near the open end of an 8-mm waveguide where mw radiation propagates in the TE$_{10}$-mode (the mw electric field $\varepsilon_{mw} \| y$), as shown schematically in Fig. 1a. $\varepsilon_{mw}$ was polarized in the sample plane and did not vary in the $y$-direction.[16] The external magnetic field was applied perpendicularly to the sample plane $B \| z$. The sample was immersed in liquid He at temperature $T_L$ = 2.1 - 4.2 K. A Gunn diode provided mw radiation of frequency $\omega = 2\pi f$, with $f$ in the range of (33 - 36.7) GHz and mw power $P_{mw}$ = 0.1-20 mW.

The sample was photoexcited with a laser diode (pho-

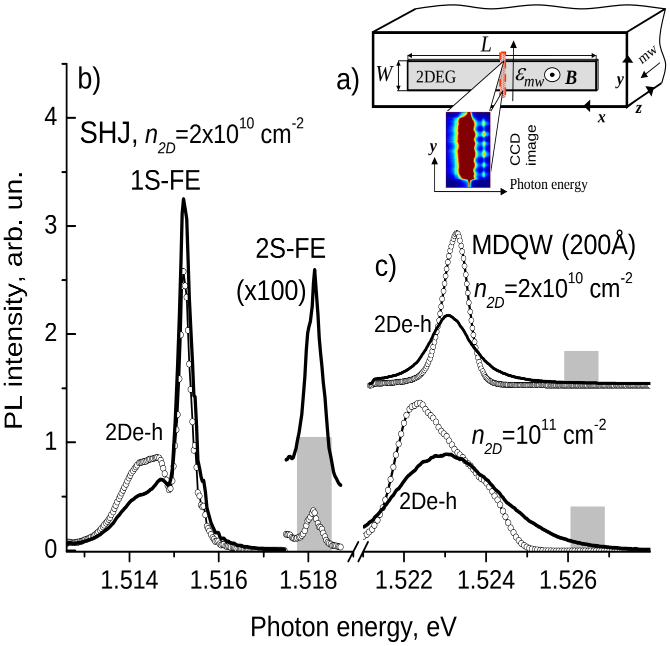


FIG. 1: a. The schematic drawing of the experiment. b,c. The photoluminescence spectra of the SHJ (b) and the 20 nm - wide MDQW (c) for $P_{mw}$=0 (curves with circle symbols) and for $P_{mw}$=10 mW (solid curves). $T_L$ = 4.2 K.

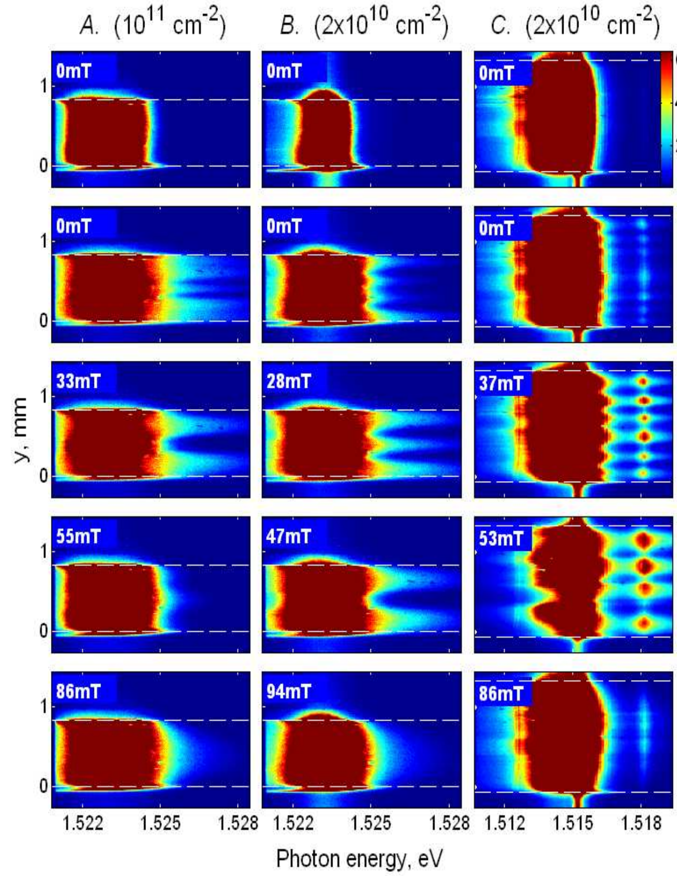


FIG. 2: The PL images obtained for the MDQW (bar width, $W$=0.85 mm) at two $n_{2D}$-values (columns $A$, $B$) and for the SHJ sample of $W$=1.3 mm (column $C$). Row 1 displays the images obtained at $P_{mw}$= 0 and $B$ = 0. The images in rows 2-5 were obtained under various $P_{mw}$-values and for the $B$-values given in Fig. The PL intensity color map is shown in row 1 (column $C$). Dashed lines show the sample borders

ton energy of $E_L = 1.56$ eV, below the $Al_xGa_{1-x}As$ barrier bandgap) with light intensity below 10 mW/cm$^2$. This photoexcitation did not affect the 2DEG properties (density and mobility). The 2DEG density was varied by optical depletion using a He-Ne laser excitation ($E_L$ = 1.96 eV).[7] PL imaging was done by focusing the diode laser beam onto a vertical strip (height $\simeq$ 2 mm and width $\simeq$ 0.25 mm) on the sample surface. The PL from the photoexcited strip was optically magnified and imaged on the spectrometer slit, dispersed in the horizontal direction and projected on a CCD matrix. The image on the CCD plane was both spatially-resolved (in the transverse $y$-direction, across the bar) and spectrally-resolved, with resolutions of $\sim$ 10$\mu$m and 0.1 meV, respectively. The longitudinal spatial resolution of $\sim$ 50$\mu$m (in the $x$-direction, along the bar) was limited by the spectrometer slit width.

The effect of mw-irradiation on the spatially-integrated PL spectra is demonstrated for a GaAs/AlGaAs SHJ sample (Fig. 1b) and for a MDQW sample (Fig. 1c). The SHJ PL spectrum consists of free exciton (FE) 1S and 2S lines. These originate in the wide GaAs buffer layer. In addition, there is a weak, broad, low-energy PL band due to the radiative recombination of 2D-electrons near the interface with free holes (2De-h PL).[7,17] Under mw irradiation, the 1S and 2S FE PL intensities strongly increase (solid curves) as compared to those at $P_{mw}$=0 (curves with circle symbols).[7,18] For the MDQW sample, 2De-h PL spectra are shown for two 2DEG density values (Fig.1c). Under mw irradiation, the spectra broaden, and the PL intensity increases at high photon energies (gray-colored area), as compared to the spectra observed at $P_{mw}$ = 0. The mw induced changes in the 2De-h and excitonic PL spectra that are shown in Figs. 1b,c are due to mw-heating of the 2D-electrons.[7–9,18–20]

Fig. 2 shows the PL spectral variations along the excitation strip ($y$-direction) as imaged through the spectrometer. In order to enhance the image contrast in the high-energy part of spectra, the PL intensity signal was amplified (so that the PL intensity at low energies is saturated) and in addition, the images were obtained at different $P_{mw}$. Columns $A$ and $B$ show PL images of a 0.85 mm-wide MDQW sample that were obtained for two $n_{2d}$-values. The PL images shown in column $C$ were measured with a 1.3 mm-wide SHJ sample. Without mw irradiation (Fig. 2, first row) the PL spectra do not vary in the $y$-direction, and the images are spatially uniform.

A PL variation along the $y$-direction emerged under mw-irradiation. In particular, the PL spectral width changes irregularly as seen in Fig. 2 row 2, column $A$. When the 2DEG density was tuned by optical depletion, a remarkable spatially-periodic oscillations appear at certain $n_{2d}$-values (Fig. 2 row 2, column $B$ and $C$). The spatial period decreases with decreasing $n_{2d}$ (Fig. 2, columns $A$ and $B$). For a given $n_{2d}$, the spatial periodicity disappears with increasing $B$, and re-emerges at certain $B$-values. The spatial period increases as $B$ increases (Fig. 2, rows 3-5). Varying $P_{mw}$ does not affect the spatial period. The most noticeable spectral changes seen in Fig.2 occur at high emission energies. In particular, we observe that the 2S FE line (at 1.518 eV) in the SHJ sample is a sensitive probe of the mw-induced changes in the 2DEG due to the remote interaction between the 2DEG and the excitons.[7,17]

The physical mechanisms causing the mw-induced changes in the PL spectra were previously studied, and these result from an increased 2D-electron temperature $T_e$.[7,18–20] Therefore, we attribute the pronounced spatial modulation of the PL spectrum to a lateral variation of $T_e(y)$ arising under mw-heating. Because $T_e$ increases proportionally to the local $|\varepsilon_{mp}(y)|^2$ (for $T_e \geq 2$ K [21,22]) the $\varepsilon_{mp}(y)$-dependence can be extracted from the PL image. Indeed, $\varepsilon_{mp}(y)$ heats the 2D-electrons locally, giving rise to a $T_e(y)$ distribution. The decay length of $T_e$ can be estimated as $\sim v_F\tau_E \sim 10$ $\mu$m (here, $v_F \sim 10^6$ cm/sec and $\tau_E \sim 10^{-9}$ sec are the electron Fermi velocity and energy relaxation time, respectively). Since this length is small relative to the the $\varepsilon_{mp}(y)$ wavelength, the $T_e(y)$ distribution closely follows the $\varepsilon_{mp}(y)$ dependence. Thus, the PL imaging in the presence of mw-irradiation allows us to obtain the spatial $\varepsilon_{mp}$-distribution in the excited MP modes, while the external mw-field $\varepsilon_{mw}(y)$ is uniform.[16]

The observed spatial periodicity of the mw-induced PL spectrum modulation indicates that $\varepsilon_{mp}$ has a periodic distribution that is a specific to each MP mode excited in the 2DEG plane by microwaves. For some $B$ and $n_{2d}$ values, more than one MP-mode can be simultaneously excited. Then, a superposition of MP-modes gives rise to a spatially irregular PL modulation as observed in Fig.2 row 2, column $A$ ($n_{2d}$=$10^{11}$ cm$^{-2}$, $B$=0).

PL imaging was also performed along the sample bar (in the $x$-direction), and a strongly non-uniform distribution of $T_e(x)$ was observed. We attribute this $T_e(x)$ dependence to the non-uniform $\varepsilon_{mp}(x)$ that is due to excitation of high-order longitudinal MP-modes along the bar.

The intensity of the high-energy spectral part of the 2De-h PL in MDQWs as well as that of the 2S exciton line in SHJ increases monotonically with increasing local $T_e \propto |\varepsilon_{mp}|^2$. Thus, the spatial profile of the mw-induced PL is used to map the MP-electric field with sub-mw-wavelength resolution. Fig. 3 shows the variation of the PL intensity (integrated over the energies marked by gray blocks in Fig. 1) across several MDQW bars. Thus, these traces display the $|\varepsilon_{mp}(y)|^2$-distribution in the 2DEG plane.

The two lower traces in Fig. 3a were obtained for two $P_{mw} = 1$ and 4 mW at $B = 0$. They show that $|\varepsilon_{mp}(y)|^2$ corresponds to a confined MP-polariton transverse mode having $q \sim 4\pi/W$ ($N = 4$). The mode patterns are independent of mw power, and increasing $P_{mw}$ causes a saturation of the peak intensities and a smearing of the spatial PL profile. The other three curves in Fig.3a are maps of $|\varepsilon_{mp}|^2$ of the MP modes excited for several magnetic field strengths. These curves show that transverse MP modes with $N = 3$, 2 and 1 are excited as $B$ increases. Note that $\varepsilon_{mp}$ almost vanishes at the sample edges which corresponds to the boundary condition for excitation of MP standing waves.[23]

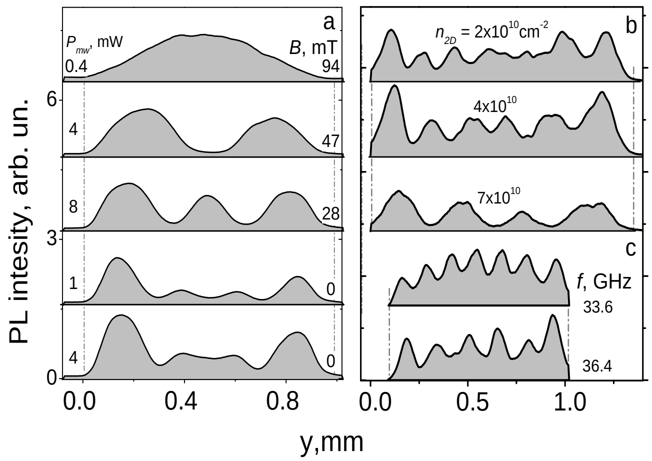


FIG. 3: Spatial profiles mapping the electric microwave field distribution in the magnetoplasmon modes: (a) $n_{2d} = 2{\cdot}10^{10}$ cm$^{-2}$ , $f = 36$ GHz for several $B$-values; (b) $B = 0$, $f = 36$ GHz for several $n_{2d}$-values; (c) $n_{2d} = 2{\cdot}10^{10}$ cm$^{-2}$ , $B = 0$ for two mw-frequencies. Dashed lines show the sample borders.

Fig. 3b maps the $|\varepsilon_{mp}(y)|^2$ dependence at $B = 0$ for several 2DEG densities tuned by optical depletion ($n_{2d}$ was estimated independently from 2De-h PL spectral width at $P_{mw} = 0$). Fig. 3c demonstrates the effect of varying the mw-frequency on the $\varepsilon_{mp}$ distribution. The $|\varepsilon_{mp}|^2$ profiles shown in Figs. 3a, b, c yield the confined MP-mode wavelength dependence on $B$, $n_{2d}$ and $f$ that corresponds qualitatively to Eqs. 1 and 2.

For the transverse MP modes, the dispersion relation is given by Eq. 2 and can be presented as:

$$\lambda = 2\pi/q = (2\pi e)^2 n_{2d}/[\omega^2 \varepsilon m^*(1 - (\omega_c/\omega)^2)] \quad (3)$$

In Fig. 4, circles show the MP wavelength $\lambda = 2W/N$ obtained from the PL pattern (as in Fig. 3) measured at $B$-values when the PL spectral broadening reaches its maximum. The measured dispersion of the transverse MP modes is well fitted by the solid curve that displays the dependence given by Eq. 3. These measurements were performed on a narrow ($W = 0.5$ mm, $L = 3$ mm) sample bar ($L \gg W$) where excitation of high order longitudinal modes in the $x$-direction, is impeded. Here, we do not consider the effects of retardation on the MP dispersion[9] because these are unimportant for low 2DEG densities.[23]

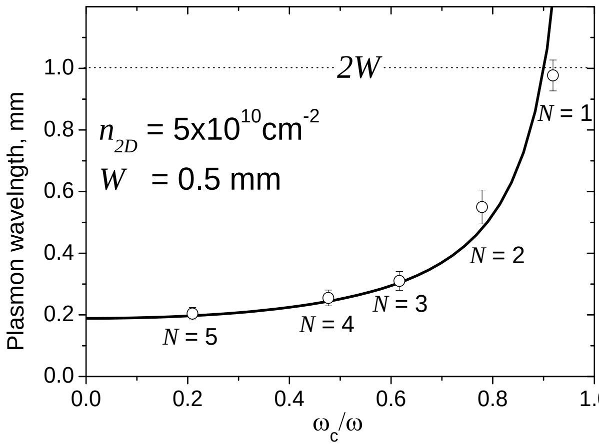


FIG. 4: The MP-wavelength dependence on magnetic field. The error bars show inaccuracy of the measurements. Solid line displays the dependence given by Eq.3

Thus, mw-irradiation of the sample generates strongly non-uniform distribution of the internal mw field $\varepsilon_{mp}(x,y)$ that varies with the magnetic field. Our study was carried out under the same conditions (in particular, the sample properties and geometry of the experiment) as those used in MIRO experiments. We propose that the observed spatial variations of $|\varepsilon_{mp}|$ and $T_e$ should be incorporated in the MIRO physical mechanism which is now under intensive discussion (see Refs list in [10,13,24]). The reason is that in measuring mw-photoresistance the integrated effect of the $\varepsilon_{mp}(x,y)$ and $T_e(x,y)$-distributions is probed. While writing this manuscript we became aware of Mikhailov's paper[13] where the MIRO is explained by a 2DEG density modulation on the micron-wide ranges near the metal contacts as a result of a strongly-inhomogeneous $|\varepsilon_{mp}|^2$.

It should be noted that the MP modes could be imaged only in the highest mobility 2DEG samples ($\mu_e \geq 2\cdot 10^6$ cm$^2$/V·s). In samples of lower mobility (below $10^6$ cm$^2$/V·s), a uniform PL modulation was observed. This is probably due to a large broadening of the MP modes and could explain the absence of the MIRO in low mobility 2DEG samples.

In conclusion, we present, for the first time, optical imaging of the internal electric field for magnetoplasmons that are excited by microwaves in a laterally confined two dimensional electron gas. This was done by monitoring the mw-induced spatial and spectral photoluminescence variation. Non-uniform patterns of the local internal microwave electric field $\varepsilon_{mp}(x,y)$ were observed, and they are due to excitation of high-order magnetoplasmon modes. Therefore, the $\varepsilon_{mp}(x,y)$ - inhomogeneity as well as the non-uniform local electron temperature distribution that arises under increased mw-power, should be considered as a central factor in the research of microwave induced effects in a 2DEG (such as MIRO and optically detected magnetoplasmon resonances).

**Acknowledgments**

The work was done in the Barbara and Norman Seiden Center for Advanced Optoelectronics at Technion. It was supported by the Israel-US Binational Science Foundation (BSF), Jerusalem and partially funded by the Gordon and Betty Moore Foundation as well as the National Science Foundation MRSEC Program through the Princeton Center for Complex Materials (DMR-0819860).

1. F. Stern, Phys. Rev. Lett. 18, 546 (1967)
2. V. A. Volkov and S. A. Mikhailov, Sov. Phys. JETP 67, 1639 (1988)
3. S. J. Allen, H.L. Stormer, J.C.M. Hwang, Phys. Rev. B 28, 4875 (1983)
4. E. Vasiliadou, et. al., Phys. Rev. B 48, 17145 (1993)
5. W. Hansen, J. P. Kotthaus, and U. Merkt, in Semiconductors and Semimetals, edited by M. Read (Academic Press, New York, 1992), Vol. 35, p. 279.
6. B. M. Ashkinadze, V. I. Yudson, Phys. Rev. Lett. 83, 812 (1999); B. M. Ashkinadze, A. Nazimov, E. Cohen, A. Ron, L. N. Pfeiffer, Phys. Status Solidi A 164, 523 (1997)
7. B. M. Ashkinadze, E. Linder, V. Umansky, Phys. Rev. B 62, 10310 (2000)
8. M. Yu. Akimov, et al., Pis'ma Zh. Eksp. Teor. Fiz. 72, 662 (2000) JETP Lett. 72, 460 (2000)
9. I.V.Kukushkin, et. al., Phys. Rev. Lett., 90, 156801 (2003) *ibid* Phys. Rev. B, 73, 113310,(2006)
10. A.T. Hatke, M.A. Zudov, L.N. Pfeiffer, K.W. West, Phys. Rev. B, 83, 121301(R) (2011)
11. S.A. Mikhailov Phys. Rev. B 70, 165311, (2004)
12. S. A. Studenikin, et. al., Phys. Rev. B 76, 165321 (2007)
13. S.A. Mikhailov Phys. Rev. B 83, 155303, (2011)
14. W. L. Barnes, et. al., Nature, 424, 824 (2003)
15. H. Ditlbacher, et. al., Applied Physics Letters, 80, 404 (2002)
16. L. Diener, Res. in Nondestr. Eval., 7, 137,(1995)
17. B. M. Ashkinadze,V. Voznyy, E. Cohen, A.Ron, V. Umansky Phys. Rev. B 65, 073311 (2002); B. M. Ashkinadze, E. Linder, E. Cohen, V. V. Rudenkov, P. C. M. Christianen, J. C. Maan, L. N. Pfeiffer, *ibid* 72, 075332 (2005)
18. I. Baskin, et. al., Phys. Stat. Sol. (c), 5, 131 (2008)
19. B. M. Ashkinadze, E. Linder, E. Cohen, L.N. Pfeiffer, Phys. Rev. B 74, 245310 (2006)
20. I. Baskin, B. M. Ashkinadze, E. Cohen, L. N. Pfeiffer, Phys. Rev. B 78, 195318 (2008)
21. B.K. Ridley, Rep. Prog. Phys. 54, 169 (1991)
22. B. M. Ashkinadze, A.V. Subashiev, JETF Lett., 46, 357 (1987)
23. S. A. Mikhailov and N. A. Savostianova, Phys. Rev. B 71, 035320 (2005)
24. I. V. Andreev, V. M. Muravev , I. V. Kukushkin , S. Schmult and W. Dietsche, Phys. Rev. B 83, 121308(R) (2011)